Rates of Oxygen and Hydrogen Exchange as Indicators of TPQ Cofactor Orientation in Amine Oxidases†

Edward L. Green,‡ Nobuhumi Nakamura,‡,§ David M. Dooley,|| Judith P. Klinman,⊥ and Joann Sanders-Loehr*,‡

Department of Biochemistry and Molecular Biology, OGI School of Science and Engineering, Oregon Health and Science University, Beaverton, Oregon 97006-8921, Departments of Chemistry and Molecular and Cell Biology, University of California, Berkeley, California 94720, and Department of Chemistry and Biochemistry, Montana State University, Bozeman, Montana 59717

Received August 20, 2001

ABSTRACT: This study presents the first detailed examination by resonance Raman (RR) spectroscopy of the rates of solvent exchange for the C5 and C3 positions of the TPQ cofactor in several wild-type copper-containing amine oxidases and mutants of the amine oxidase from *Hansenula polymorpha* (HPAO). On the basis of crystal structure analysis and differing rates of C5═O and C3−H exchange within the enzyme systems, but equally rapid rates of C5═O and C3−H exchange in a TPQ model compound, it is proposed that these data can be used to determine the TPQ cofactor orientation within the active site of the resting enzyme. A rapid rate of C5═O exchange ($t_{1/2}$ < 30 min) and a slow ($t_{1/2}$ = 6 h) to nonexistent rate of C3−H exchange was observed for wild-type HPAO, the amine oxidase from *Arthrobacter globiformis*, pea seedling amine oxidase at pH 7.1, and the E406Q mutant of HPAO. This pattern is ascribed to a productive TPQ orientation, with the C5═O near the substrate-binding site and the C3−H near the Cu. In contrast, a slow rate of C5═O exchange ($t_{1/2}$ = 1.6−3.3 h) coupled with a fast rate of C3−H exchange ($t_{1/2}$ < 30 min) was observed for the D319E and D319N catalytic base mutants of HPAO and for PSAO at pH 4.6 ($t_{1/2}$ = 4.5 h for C5═O exchange). This pattern identifies a flipped orientation, involving 180° rotation about the Cα−Cβ bond, which locates the C3−H near the substrate-binding site and the C5═O near the Cu. Finally, fast rates of both C5═O and C3−H exchange ($t_{1/2}$ < 30 min) were observed for the amine oxidase from *Escherichia coli* and the N404A mutant of HPAO, suggesting a mobile cofactor, with multiple TPQ orientations between productive and flipped. These results demonstrate that opposing sides of the TPQ ring possess different degrees of solvent accessibility and that the rates of C5═O and C3−H exchange can be used to predict the TPQ cofactor orientation in the resting forms of these enzymes.

Copper amine oxidases, found in bacteria, fungi, plants, and mammals (*1*), catalyze the oxidative deamination of a primary amine to its corresponding aldehyde and ammonia, with concomitant reduction of molecular oxygen to hydrogen peroxide. These enzymes allow prokaryotes to use primary amines as a carbon and nitrogen source. The actual functions in eukaryotes are unclear, but they are believed to be involved in cell signaling, growth, and development. A recent study has implicated a cell-surface amine oxidase in the control of lymphocyte migration (*2*). Most copper-containing amine oxidases possess the same self-processed organic cofactor, 2,4,5-trihydroxyphenylalanine quinone (TPQ)[1] (*3*). Formation of the TPQ cofactor by the post-translational modification of a tyrosine residue within the active site consensus sequence T-X-X-N-Y*-D/E involves self-processing events requiring only copper and molecular oxygen (*4*−*7*).

X-ray crystal structures are now available for the copper-containing amine oxidases from yeast, *Hansenula polymorpha* (HPAO) (*8*), *Escherichia coli* (ECAO) (*9*), pea seedling (PSAO) (*10*), and *Arthrohacterglohiformis* (AGAO) (*11*). Each of these enzymes is a homodimer with subunit molecular masses of approximately 80 kDa. The structure of each subunit is dominated by β sheets in a large catalytic domain and two or three smaller peripheral domains. The active site pocket contains a square pyramidal Cu^{II} ion bound by three His residues and two water molecules. In HPAO, the Cu^{II} ion is located near the C2 carbonyl oxygen of the TPQ organic cofactor (*8*). An Asp residue at position 319, part of the active site, is located on the opposite side of the TPQ cofactor near the C5 carbonyl oxygen (Figure 1). A detailed mechanism has been proposed on the basis of X-ray crystal structures (*8*−*13*) and model studies (*14*, *15*). Substrate oxidation is initiated by covalent addition of amine substrate to the C5 position of the cofactor. After proton

† This work was supported by grants from the NIH (GM 34468 to J.S.-L., GM 27659 to D.M.D., and GM 39296 to J.P.K.).

* To whom correspondence should be addressed. Phone: (503) 748-1074. Fax: (503) 748-1464. E-mail: joann@bmb.ogi.edu.

‡ Oregon Health and Science University.

§ Present address: Department of Biotechnology, Tokyo University of Agriculture and Technology, Koganei, Tokyo 184-8588, Japan.

|| Montana State University.

⊥ University of California.

[1] Abbreviations: RR, resonance Raman; HPAO, amine oxidase from *H. polymorpha*; AGAO, amine oxidase from *A. globiformis*; ECAO, amine oxidase from *E. coli*; PSAO, amine oxidase from pea seedlings; TPQ, 2,4,5-trihydroxyphenylalanine quinone; C5═O, carbonyl oxygen at the C5 position of the TPQ ring; C3−H, hydrogen at the C3 position of the TPQ ring; $tBQO^-$, 2-hydroxy-5-*tert*-butyl-1,4-benzoquinone, ionized form.

10.1021/bi011685y CCC: $22.00
Published on Web 12/13/2001

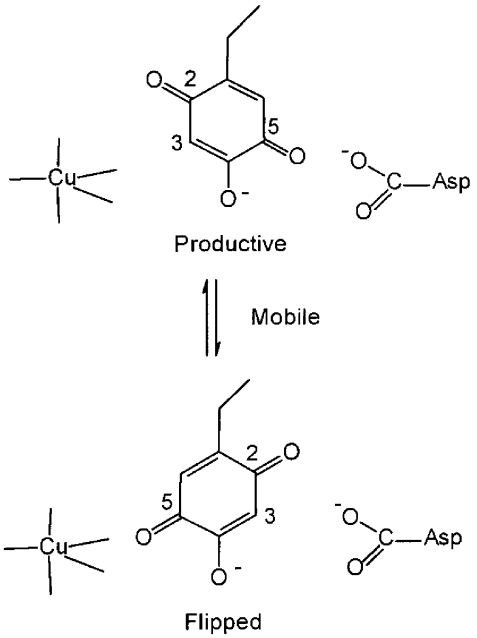

FIGURE 1: TPQ orientations observed in crystal structures of amine oxidases. Well-defined electron densities identify a productive orientation for the TPQ ring in HPAO at pH 6.3 (*8*), and a flipped orientation for the TPQ ring in PSAO at pH 4.8 (*10*). ECAO at pH 7.1 has poorly resolved electron density suggesting a mobile cofactor with multiple orientations (*9*).

abstraction from the substrate Schiff base complex by the catalytic base, the product imine is hydrolyzed to release product aldehyde. Oxidation of the aminoquinol cofactor by O_2 produces the iminoquinone, which is hydrolyzed to the release product ammonia.

A wealth of data suggests that the TPQ ring is mobile and can adopt various positions and orientations within the active site leading to differences in enzyme activity. The crystal structure of HPAO (*8*) shows the TPQ cofactor in a productive orientation with its C2 carbonyl oxygen directed toward the Cu via a H-bond to a water ligand and the C5 carbonyl oxygen pointed toward Asp 319 and the substrate-binding pocket (Figure 1). A bridging water molecule is believed to form hydrogen bonds between the C5 carbonyl oxygen and the catalytic base. In contrast, the PSAO structure at pH 4.8 (*10*) reveals that the TPQ cofactor rests in a flipped (nonproductive) orientation, with the C5 carbonyl oxygen directed toward the Cu and away from the active site base (Figure 1). In HPAO, mutation of Glu 406 (which flanks the cofactor toward the C-terminus) to Asn leads to the accumulation of the product Schiff base intermediate when methylamine is the substrate (*16*). This phenomenon is attributed to a rotation of the cofactor−product imine complex to a flipped orientation that is incompetent toward hydrolysis. A similar inactivation with methylamine as a substrate occurs upon mutation of Asn 404 (which flanks the cofactor toward the N-terminus) to Ala in HPAO (*17*). Again, this phenomenon of inactivation is believed to arise from cofactor flipping during turnover, thus shielding the product Schiff base from hydrolysis. Finally, it is also likely that rotation of the TPQ ring occurs during biogenesis of the cofactor (*5*, *11*).

Can the orientation of the TPQ cofactor in the resting form of the enzyme be predicted? In previous studies of ECAO and AGAO, we showed that the oxygen at the C5 position and the hydrogen at the C3 position of the TPQ cofactor are capable of exchanging with solvent water (*3*, *18*, *19*). Insertion of heavier isotopes (^{18}O or D) causes C═O and C−H vibrational modes to shift to lower energy, thereby affording the possibility of using resonance Raman (RR) spectroscopy to measure the rates of exchange (*18*, *19*). Since the substrate-binding channel is likely to be most accessible to solvent, we propose that the TPQ C5 carbonyl oxygen and C3 hydrogen should show different rates of exchange depending on which edge of the TPQ ring is facing the catalytic base. If the cofactor is in a productive conformation (Figure 1), then the C5 carbonyl exchange rate should be fast and the C3 hydrogen exchange rate should be slow. If the cofactor is in a nonproductive conformation, then the C5 carbonyl exchange rate should be slow and the C3 hydrogen exchange rate should be fast. Finally, fast exchange of both the C5 carbonyl and C3 hydrogen would suggest a dynamic state with the TPQ ring rapidly flipping between both conformations, corresponding to a disordered TPQ ring in the X-ray crystal structure (*9*, *13*).

Our present studies of the wild-type (WT) forms of HPAO, PSAO, ECAO, and AGAO reveal a strong correlation between the observed rates of C5═O and C3−H exchange and those expected on the basis of cofactor orientation in crystal structures. We have also analyzed oxygen and hydrogen exchange rates in several mutants of HPAO with altered enzymatic activities: two catalytic base mutants, D319N and D319E, and two mutants of the residues flanking the TPQ cofactor, N404A and E406Q. Both of the catalytic base mutants generate TPQ; however, D319N does not turn over substrates, and D319E turns over substrates at a rate 100-fold slower than that in the wild type (*20*). For the other two mutants, both E406Q and N404A generate active TPQ cofactors, but the N404A mutant turns over substrate 1000-fold slower than WT-HPAO (*17*). In each case, we found that the C5═O and C3−H exchange rates measured using RR spectroscopy correlate with differences in enzyme reactivity and, thus, allow us to predict the orientation of the TPQ cofactor.

EXPERIMENTAL PROCEDURES

Protein Preparation. Wild-type HPAO and the HPAO mutants (D319E, D319N, N404A, and E406Q) were prepared as previously described (*17*, *20*, *21*). The amine oxidase gene from *H. polymorpha* was inserted and expressed in *Saccharomyces cerevisiae* or *E. coli* (E406Q). Wild-type HPAO in 50 mM potassium phosphate (pH 7.0) was concentrated to 0.4−2.6 mM in TPQ using a Microcon 30 (Amicon) ultrafiltration device. Solutions of mutant enzymes were similarly concentrated to 0.7−0.8 mM in TPQ. Wild-type ECAO and AGAO (phenethylamine oxidase) were prepared as ∼1 mM protein solutions in 0.05 M potassium phosphate (KP_i) (pH 7.1) (*18*, *19*). Wild-type PSAO was purified as described previously (*22*) and prepared in 0.1 M KP_i (pH 7.2) or 0.01 M sodium acetate (pH 4.6) at a concentration of 1 mM protein.

Resonance Raman Spectroscopy. RR spectra were collected on a McPherson 2061 spectrograph (0.67 m, 1800-groove grating) using a Kaiser Optical holographic super-notch filter and a Princeton Instruments (LN-1100PB) liquid N_2-cooled CCD detector. The excitation source was a

Coherent Innova 90-6 Ar laser. Spectra were collected from samples contained in glass capillary tubes, cooled to ice temperature in a copper coldfinger (*23*), using 514.5 nm excitation (100 mW), 90° scattering geometry, 4 cm^{-1} spectral resolution, and 10 min accumulations (unless otherwise stated). Peak frequencies were calibrated relative to an indene standard and are accurate to ± 1 cm^{-1}. In cases where peaks are overlapping, reported peak frequencies and intensities are based on a peak-fitting procedure for curve resolution. Spectra of samples substituted with isotopes were obtained under identical instrumental conditions such that frequency shifts are accurate to ± 0.5 cm^{-1} (*23*).

Isotope Exchange in WT-HPAO and Mutants. Because of protein instability under ambient conditions, exchange experiments and Raman spectroscopy were performed on samples at 5 °C. For studying rapid ^{18}O exchange in WT-HPAO, 10 μL of concentrated HPAO (2.6 mM TPQ) was diluted with an equal amount of 50 mM KP_i (pH 7.0) in 93% $H_2{}^{18}O$ and immediately transferred to a capillary tube. This allowed a RR spectrum to be obtained within 1 min of addition of $H_2{}^{18}O$ buffer. To obtain more complete ^{18}O exchange at the C5 carbonyl oxygen, HPAO (0.4 mM TPQ) was diluted 20-fold with 50 mM KP_i in 93% $H_2{}^{18}O$ (pH 7.0) and then reconcentrated in a Microcon 30 device for 30−60 min to give a final TPQ concentration of 0.4 mM in ~89% $H_2{}^{18}O$. D_2O exchange was achieved by diluting WT-HPAO (0.4 mM TPQ) 20-fold in 50 mM KP_i in 95% D_2O (pH reading of 7.0) and then reconcentrating in a Microcon 30 device to give a final TPQ concentration of 0.4 mM in ~90% D_2O. Due to the difficulty of obtaining concentrated solutions of the D319E, D319N, N404A, and E406Q mutants of HPAO, oxygen and hydrogen exchange could only be assessed after dilution and reconcentration (as described for WT-HPAO) and, thus, were constrained by the minimum ultrafiltration time of ~1 h.

Isotope Incorporation during Biogenesis of HPAO. Apo-HPAO (0.32 mM in subunits) was prepared from *H. polymorpha* expressed in *E. coli* grown in the absence of copper (*21*) and transferred into $H_2{}^{18}O$ by diluting it 3.5-fold into 50 mM KP_i in 93% $H^{18}O$ (pH 7.0) and reconcentrating two times. Aerobic addition of $CuCl_2$ to apoHPAO, followed by mixing and incubation for 30 min at ice temperature, resulted in the formation of holo-HPAO (0.32 mM in TPQ).

Isotope Exchange in ECAO, AGAO, PSAO, and the Model Compound. Exchange experiments and Raman spectroscopy were performed at room temperature. Slowly exchanging protein samples (>1 h) were obtained by 20-fold dilution and ultrafiltration, whereas rapidly exchanging samples (<2 min) were obtained by 2-fold dilution, as described above for WT-HPAO, in $H_2{}^{18}O$ or D_2O. The ammonium salt of the model compound 2-hydroxy-5-*tert*-butyl-1,4-benzoquinone (tBQOH) was synthesized according to the previously published procedures (*14*) and dissolved in 25 mM NaP_i (pH 7.1) to yield a 20 mM solution. Deuterium exchange was initiated by a 10-fold dilution in 50 mM NaP_i (pH reading of 7.1) in D_2O.

Exchange Rate Calculation. For the HPAO mutants, 15 min scans were taken repeatedly during the first 2 h of ^{18}O exchange and then reduced to one scan every hour. After 5 h, one scan was taken every 2−4 h until the exchange reached completion. The total elapsed time was calculated to the midpoint (7 min) of each 15 min scan. Interfering vibrational modes from the apoprotein and water were subtracted from each spectrum to isolate the C5 carbonyl stretches (*19*). In each case, peak intensities (heights) were calculated for the C5═^{18}O stretch at 1650 cm^{-1} and the C5═^{16}O stretch at 1680 cm^{-1}. The fraction exchanged (F) was obtained from the ratio of peak intensities via $[I_{1650}/(I_{1650} + I_{1680})]/[I_{650}$ at completion$/(I_{1650} + I_{1680}$ at completion$)]$. The rate of ^{18}O exchange was obtained by fitting the plot of F versus time after ^{18}O addition to the equation $F = ae^{-kt}$, where a is a constant and k is the rate constant. This equation is a version of the integrated rate law, $[A] = [A]_0e^{-kt}$. The exchange reaction half-life was calculated using the formula $t_{1/2} = (\ln 2)/k$, assuming a first-order reaction. A similar treatment was used for the D- or ^{18}O-sensitive peaks in the RR spectra of the wild-type amine oxidases.

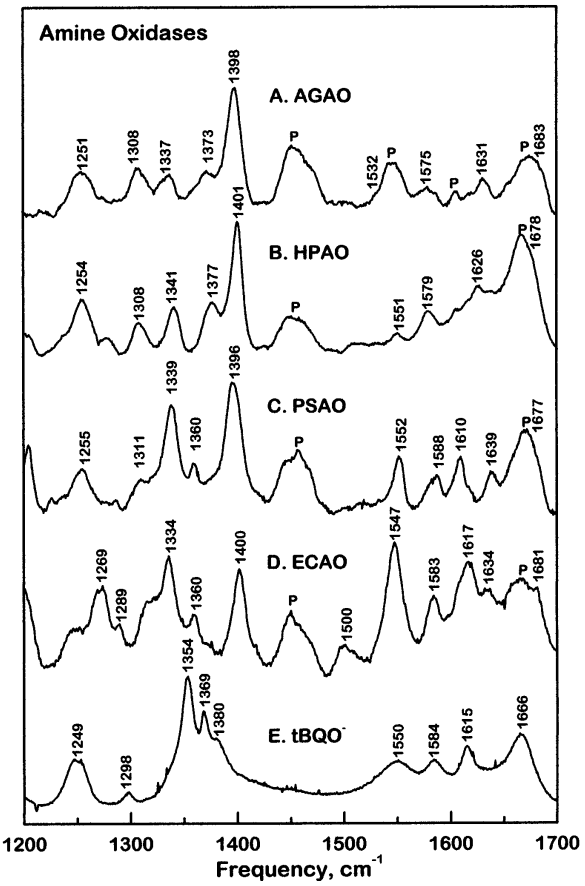

FIGURE 2: Resonance Raman spectra of copper-containing amine oxidases and models. (A) Phenethylamine oxidase (1.3 mM) from *A. globiformis* in 50 mM HEPES (pH 6.8). (B) Amine oxidase (1.3 mM) from *H. polymorpha* in 50 mM phosphate (pH 6.8). (C) Pea seedling amine oxidase [1.4 mM in 100 mM phosphate (pH 7.2)]. (D) Amine oxidase (0.4 mM) from *E. coli* in 50 mM phosphate (pH 7.0). (E) $tBQO^-$ model compound (~2 mM) in aqueous solution (pH 9.6). Data from published spectra of AGAO (*19*), HPAO (*24*), PSAO (*24*), ECAO (*18*), and $tBQO^-$ (*18*). P denotes a protein vibrational mode.

RESULTS

Raman Spectra of Amine Oxidases. Excitation of WT-HPAO within its 480 nm absorption band produces a RR spectrum characteristic of the TPQ chromophore (Figure 2B). The large number of vibrational modes between 1200 and 1700 cm^{-1} are due to a combination of C═C, C−C, and

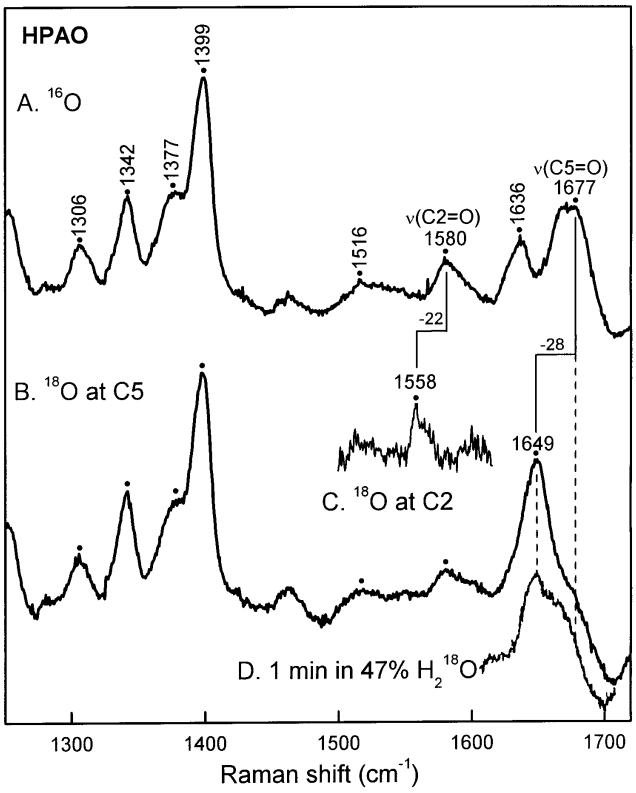

FIGURE 3: Effect of oxygen isotopes on the Raman spectrum of WT-HPAO. Spectral contributions from protein Raman modes were removed by subtracting the spectrum of the apoprotein. (A) HPAO in $H_2{}^{16}O$. (B) HPAO incubated for 1 h in 89 at. % ^{18}O. (C) Biogenesis of HPAO in $H_2{}^{18}O$. (D) HPAO in $H_2{}^{16}O$ diluted with $H_2{}^{18}O$ to yield 47 at. % ^{18}O. The spectrum (20 s accumulation) was obtained within 1 min of mixing.

C═O stretching and C−H bending modes of the TPQ cofactor. A similar RR spectral pattern is observed for other copper amine oxidases, including ECAO, PSAO, and AGAO, as well as a TPQ model compound (Figure 2). All of the protein spectra have their most intense vibrational feature near 1400 cm^{-1}, in addition to other significant features near 1340, 1375, 1580, 1635, and 1680 cm^{-1}. The shifting of the most intense feature to 1354 cm^{-1} in the model compound (Figure 2E) is most likely due to its greater charge delocalization (see below). Upon incubation in $H_2{}^{18}O$, the peaks at 1681, 1683, and 1666 cm^{-1} in ECAO, AGAO, and the $tBQO^-$ model, respectively, downshift by ∼25 cm^{-1}, leading to their assignment as the C5═O stretch (*18*, *19*). The similarity of the RR frequencies and intensities among the amine oxidases suggests that a similar electronic structure and resonance stabilization is common to all of their TPQ moieties and that this electronic structure is not significantly perturbed by the different TPQ orientations seen in the crystal structures.

The C5═O stretching mode in the RR spectra of amine oxidases is obscured by intense protein (amide I) vibrational modes in this region (Figure 2). Subtraction of the Raman spectrum of apoHPAO, obtained from Cu-deficient organisms prior to TPQ formation (*21*), yields improved definition of the C5═O stretch at 1677 cm^{-1} in WT-HPAO (Figure 3A). A clear identification of this vibration is obtained by observing its downshift to 1649 cm^{-1} upon incubation in $H_2{}^{18}O$ (Figure 3B). The magnitude of the shift (−28 cm^{-1}) indicates that only one oxygen atom in the TPQ ring has been replaced by ^{18}O. A similar downshift of −23 cm^{-1} is observed for the 1666 cm^{-1} peak in the $tBQO^-$ model in $H_2{}^{18}O$ and is accompanied by an increase of 2 mass units according to mass spectrometry (*18*).

Scheme 1: Proposed Mechanisms for H and O Exchange on TPQ

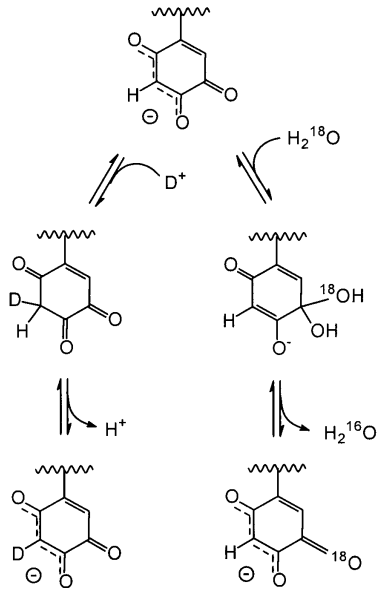

A probable pathway for C5═O exchange is shown in Scheme 1. Exchange is initiated by nucleophilic attack of the solvent at C5, leading to a dihydroxy intermediate which then reverts back to a carbonyl and accumulates the C5═^{18}O in the presence of excess ^{18}O in the solvent. Enzymatic turnover is similarly initiated by nucleophilic attack of the substrate at C5, leading to a carbinolamine intermediate which then loses H_2O to form the substrate Schiff base iminoquinone (*20*).

In a previous study of AGAO, we showed that the C2 carbonyl is derived from solvent oxygen during cofactor biogenesis and does not exchange with solvent in the fully formed cofactor (*19*). The C2═O stretch was observed at 1575 cm^{-1} in the RR spectrum of AGAO and downshifted by 21 cm^{-1} when the cofactor was generated in $H_2{}^{18}O$ (*25*). We have now observed similar results for wild-type HPAO. ApoHPAO in $H_2{}^{18}O$ was reacted with $CuCl_2$ and O_2 to promote cofactor formation. The RR spectrum shows a 22 cm^{-1} downshift for the peak at 1580 cm^{-1} (Figure 3C), as well as smaller shifts of −3 to −5 cm^{-1} for peaks at 1252, 1306, 1378, and 1398 cm^{-1}, similar to the shifts for AGAO (Table 1). These results establish the 1580 cm^{-1} mode as the predominant C2═O stretch and prove that the formation of TPQ involves the insertion of a solvent oxygen at the C2 position in HPAO. The similarity of the isotope shifts indicates that the C2═O stretch in HPAO is coupled with similar ring vibrational modes and, thus, has a degree of electron delocalization between the C2 and C4 positions similar to that in AGAO.

Rapid Isotope Exchange in the TPQ Model Compound. Exchange of the C3 hydrogen of the quinone ring with solvent deuterium has been amply demonstrated by both NMR and mass spectrometry in TPQ model compounds (*3*, *18*). The $tBQO^-$ model compound undergoes an increase of 1 mass unit in D_2O, showing that there is only one exchangeable hydrogen (*18*). A probable pathway for C3−H

Table 1: Isotope Shifts from ^{18}O Incorporation at the C2 or C5 Position of the TPQ Ring[a]

AGAO[b]			HPAO		
	$\Delta^{18}O$			$\Delta^{18}O$	
frequency	C2	C5	frequency	C2	C5
1251	−3	−1	1252	−3	0
1308	−4	−1	1306	−5	0
1337	0	0	1342	−1	0
1373	−6	0	1378	−5	0
1398	−4	−1	1398	−5	0
1532	−3	0			
1575	−21	0	1580	−22	0
1631	0	0	1636	0	0
1683	0	−27	1677	0	−28

[a] Frequencies in cm^{-1}. $\Delta^{18}O$ denotes the shift (cm^{-1}) upon substitution of ^{18}O for ^{16}O. [b] Data from ref. *24*.

Table 2: Raman Frequencies and Half-Times for Isotope Exchange in Amine Oxidases and the Model Compound[a]

	C5═O mode			C3−H mode		
sample	ν	[$\Delta^{18}O$]	$t_{1/2}$	ν	[ΔD]	$t_{1/2}$
mobile orientation						
$tBQO^-$ (pH 7.1)	1666	−23	<2 min	1354	−10	2 min
$tBQO^-$ (pH 4.0)	1666	−23	<30 min[b]			
ECAO	1681	−26	<5 min	1289	−9	0.5 min
N404A (HPAO)	1681	−22	<30 min	1298[c]		<30 min
productive orientation						
HPAO	1678	−28	<1 min	no[d]		
E406Q (HPAO)	1679	−28	<30 min	no[d]		
AGAO	1683	−27	<2 min	1308	−16	6 h
PSAO (pH 7.1)	1677	−26	2 min	no[d]		
flipped orientation						
PSAO (pH 4.6)	1677	−26	4.5 h	no[d]		
D319E (HPAO)	1681	−25	3.3 h	1298[c]		<30 min
D319N (HPAO)	1674	−22	1.6 h	1298[c]		<30 min

[a] Frequencies (ν) and isotope shifts ($\Delta^{18}O$ and ΔD) are in cm^{-1}. Exchange was assessed at 298 K for the WT enzymes and model compound and at 278 K for the HPAO mutants. Half-times ($t_{1/2}$) are based on three to five determinations and were calculated by fitting the fraction exchanged, F, to the equation $F = ae^{-kt}$, where $t_{1/2} = (\ln 2)/k$. The error range for samples with a half-life greater than 1 h is ±0.7 h. The ionic strength was held constant at ~0.1. [b] Slow dissolution prevented earlier time points. [c] Frequency in D_2O. [d] Not observed (due to a lack of exchange or a lack of resonance enhancement).

exchange is shown in Scheme 1. Charge delocalization from the oxygen at C4 into the TPQ ring facilitates proton (or deuteron) addition at the C3 position, leading to a dihydro intermediate which then dissociates to the monodeutero product in excess D_2O.

The $tBQO^-$ model compound exhibits substantial RR spectral changes in D_2O with downshifts of −25 cm^{-1} at 1298 cm^{-1} and −10 cm^{-1} at 1354 cm^{-1} (*18*). Exchange occurs rapidly upon dissolution of the solid in D_2O (pH reading of 7.1) such that the RR spectral changes are complete within 5 min. Curve resolution of the peak intensities at 1354 and 1344 cm^{-1} and a nonlinear curve fit of these intensities over time lead to a calculated $t_{1/2}$ of 2 min for D exchange in the $tBQO^-$ model compound (Table 2). A similarly rapid rate of exchange ($t_{1/2}$ < 2 min) is observed for the C5═O mode at 1666 cm^{-1} when the $tBQO^-$ model compound is dissolved in $H_2{}^{18}O$ (Table 2). These results demonstrate that both the C3−H and the C5═O of TPQ are capable of exchanging rapidly with solvent in the absence of catalysts. The occurrence of slower exchange rates for either the C3−H or C5═O in the amine oxidases (see below) can, therefore, be ascribed to the decreased solvent accessibility of the TPQ cofactor within the enzyme active site.

Rapid Isotope Exchange in ECAO. The TPQ cofactor in ECAO has facile exchange of the C3−H and the C5═O similar to that in the $tBQO^-$ model compound. The 1289 cm^{-1} peak in ECAO exhibits a deuterium isotope shift of −9 cm^{-1}, which has been ascribed to the rapidly exchanging C3 hydrogen (*18*). Quantitation of peak intensities reveals an even faster rate of D exchange in ECAO than in the model compound with a $t_{1/2}$ of 0.5 min (Table 2). Furthermore, the C5═O stretch at 1681 cm^{-1} in ECAO undergoes a shift to 1655 cm^{-1} in $H_2{}^{18}O$ with a $t_{1/2}$ of <5 min for ^{18}O exchange (Table 2). The rapid rates for both C3−H and C5═O exchange in ECAO suggest that the TPQ ring readily flips between the two orientations, in agreement with its disordered electron density in the crystal structure (*9*).

Isotope Exchange in HPAO. Exchange of the C5═O in WT-HPAO, as measured by the RR shift from 1677 to 1649 cm^{-1}, is essentially complete in the 1 h required for dilution and ultrafiltration (Figure 3B). The spectrum was unchanged after incubation for 5 h in $H_2{}^{18}O$, with the small shoulder at 1677 cm^{-1} being due to the 11% $H_2{}^{16}O$ in the sample. To obtain a closer estimate of the exchange rate, a concentrated solution of WT-HPAO was diluted 1:1 in $H_2{}^{18}O$ in buffer and a spectrum was obtained within 1 min (Figure 3D). Exchange was assessed by the new intensity at 1649 cm^{-1} and was found to be complete in this time period. The $t_{1/2}$ for this reaction is <1 min at ice temperature as well as room temperature (Table 2). The rapid exchange of the C5═O in WT-HPAO is in agreement with the productive orientation of the TPQ ring in the crystal structure (*8*). Since the C5 carbonyl is directed toward the catalytic base and the substrate-binding pocket (Figure 1), it is expected to exchange rapidly with solvent.

The RR spectrum of WT-HPAO exhibits a small peak at 1308 cm^{-1} that could be related to the 1298 cm^{-1} C3−H vibrational mode in the $tBQO^-$ model compound. However, neither this peak nor any other spectral feature of WT-HPAO changes upon prolonged incubation for hours to days in D_2O. These results imply that either the C3−H is not exchanging or vibrations of the C3−H are not resonance-enhanced (i.e. not part of the 1308-cm^{-1} vibrational motion) in WT-HPAO.

Isotope Exchange in AGAO. The X-ray structure of WT-AGAO at pH 8.1 and 2.2 Å resolution revealed clear electron density that could be attributed to the entire TPQ ring as well as the oxygens at the C2 and C4 positions, thereby indicating that the ring is in an ordered conformation (*10*). However, no density was observed for the oxygen at the C5 position, making it impossible to determine whether the ring is in a productive or flipped orientation. In contrast, the high-resolution X-ray structure of WT-ECAO at 100 K reveals only partial electron density for the TPQ ring, consistent with rotational motions and a disordered TPQ orientation (*9*). Our RR findings of fast rates of exchange for both the C5═O and the C3−H in ECAO (see above) support the crystallographic evidence for a mobile TPQ ring. Similarly, our RR investigation of AGAO points to a more ordered disposition of the TPQ ring, as suggested by the crystal structure.

AGAO is similar to ECAO in that its RR spectrum is affected by incubation in D_2O, causing a 16 cm^{-1} downshift

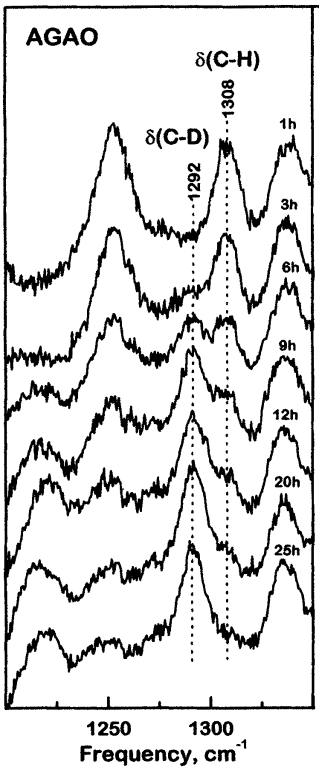

FIGURE 4: Raman spectra of AGAO as a function of time of exposure to D_2O. AGAO (1 mM in protein) in 0.05 M HEPES (pH reading of 7.1) in 94 at. % D. Spectra are for 5 min accumulations.

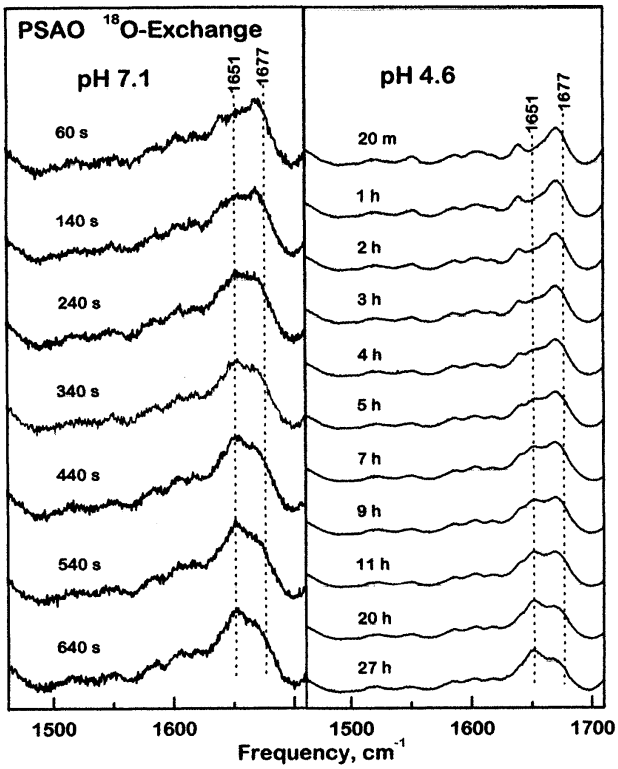

FIGURE 5: Raman spectra of PSAO as function of time of exposure to $H_2{}^{18}O$. At the left are data for 0.5 mM enzyme in 0.01 M HEPES (pH 7.1) in 50 at. % ^{18}O. Spectra are for 10 s accumulations. At the right are data for 1.0 mM enzyme in 0.01 M acetate (pH 4.6) in 81 at. % ^{18}O.

from 1308 to 1292 cm^{-1} (Figure 4), compared to the 9 cm^{-1} downshift from 1289 to 1280 cm^{-1} observed for ECAO. However, the two enzymes differ in the rate of C3−H exchange which is fast ($t_{1/2}$ = 0.5 min) for ECAO and slow for AGAO. In 0.05 M HEPES (pH 7.1) at an ionic strength of 0.09, D exchange in AGAO is complete by 20 h with a $t_{1/2}$ of 6 h (k_{obs} of 0.1 h^{-1}) (Figure 4). The rate of C3−H exchange in AGAO is inversely proportional to ionic strength such that a $t_{1/2}$ of 4 h (k_{obs} of 0.2 h^{-1}) is achieved at an ionic strength of 0.02. As in the case of HPAO and ECAO, the rate of ^{18}O exchange in AGAO is much faster ($t_{1/2}$ < 2 min) (Table 2). The slow C3−H exchange and rapid C5═O exchange in AGAO suggest that the TPQ ring is held in a productive conformation.

Isotope Exchange in PSAO. The X-ray structure of PSAO was determined on material that had crystallized at pH 4.8 (*10*). The electron density of the TPQ ring was clearly defined and shown to be in a flipped orientation with the C2═O hydrogen-bonded to Asp 300, the catalytic base. The enzyme is fairly stable at this pH and still exhibits enzymatic activity, albeit 4-fold lower than at neutral pH. The TPQ absorption maximum red shifts from 500 nm at pH 7.2 to 515 nm at pH 5.2 (*22*). Studies of the $tBQO^-$ model compound reveal that protonation of the hydroxyquinone causes the absorption maximum to blue shift from 498 to 372 nm (*14*). Thus, the red shift in the PSAO absorption spectrum at low pH is more likely due to an increase in the resonance delocalization of electrons from the C4 oxyanion through the C2═O (Scheme 1).

Additional evidence for a change in TPQ electronic structure with pH comes from RR spectroscopy. The RR spectrum of PSAO at pH 7.2 is similar to that of other amine oxidases with the most intense ring vibrational mode at 1396 cm^{-1} (Figure 2C). However, at pH 4.6 there is a marked drop in the intensity of this peak, and the peak at 1337 cm^{-1} has grown in intensity to become the dominant feature in the RR spectrum (data not shown). This RR intensity pattern is similar to that of $tBQO^-$ at neutral to alkaline pH, where the spectrum is dominated by a lower energy peak at 1354 cm^{-1} (Figure 2E). The $tBQO^-$ system is known to have strong charge delocalization in the quinone ring (*15*). An increase in the level of electron delocalization in PSAO at low pH is consistent with the observation that its TPQ ring lacks the (TPQ)C4−O···HO(Tyr) hydrogen bonding interaction (*10*) which has been observed in the crystal structures of amine oxidases at neutral pH (*8*, *9*, *11*).

A dramatic effect of pH is seen in the rates of C5═O exchange in PSAO (Figure 5). At pH 7.1, the reaction is complete in 500 s ($t_{1/2}$ = 2 min), whereas complete exchange at pH 4.6 requires 20 h ($t_{1/2}$ = 4.5 h). In contrast, the $tBQO^-$ model still undergoes a rapid ^{18}O exchange at pH 4 ($t_{1/2}$ < 30 min), indicating that the reaction is not simply limited by the lower concentration of hydroxide. The remarkably slow rate of C5═O exchange in the low-pH PSAO can, thus, be attributed to the flipped orientation of TPQ which makes C5 less accessible to solvent. The fast rate of ^{18}O exchange in PSAO at neutral pH indicates that the TPQ cofactor has shifted to the productive orientation where the C5═O is more accessible to solvent. Like HPAO, the neutral form of PSAO has a RR peak at 1311 cm^{-1} that is unaffected by incubation in D_2O, suggesting that the C3−H may not be exchanging in the productive conformation. The low-pH form of PSAO is also unaffected by incubation in D_2O; however, its lack

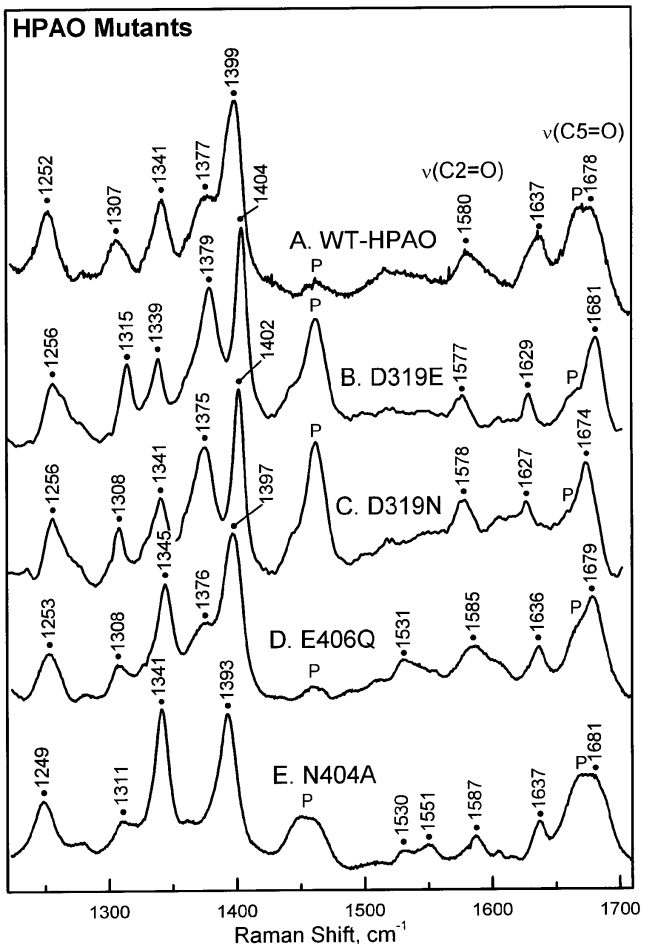

FIGURE 6: Resonance Raman spectra of (A) WT-HPAO (0.4 mM in TPQ) and the (B) D319E, (C) D319N, (D) E406Q, and (E) N404A mutants of HPAO. Mutants were 0.7−0.8 M in TPQ. P denotes a protein vibrational mode. Spectra A and D were corrected for Raman contributions due to protein and solvent. Spectra B, C, and E were corrected for Raman contributions due to solvent.

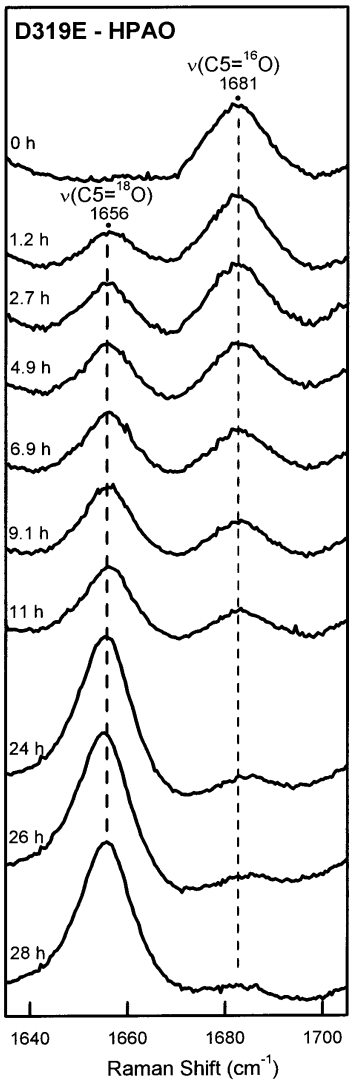

FIGURE 7: Raman spectra of the D319E mutant of HPAO (0.4 mM in TPQ) as a function of the time of reaction with $H_2{}^{18}O$ (89 at. % ^{18}O). Spectra are for 15 min accumulations and have been corrected for Raman contributions of apoHPAO and solvent.

of a RR peak near 1311 cm^{-1} suggests a lack of coupling of the C3−H mode with resonance-enhanced ring modes. The 135-fold decrease in the rate of C5═O exchange compared to only a 4-fold decrease in enzymatic activity in PSAO at low pH suggests that substrate binding promotes ring flipping to the productive orientation as in HPAO (*20*).

Isotope Exchange in Catalytic Base Mutants. In the D319E and D319N variants of HPAO, the catalytic base has been replaced by a longer chain carboxylate, which behaves as a weaker catalyst, or by an asparagine, which destroys its catalytic activity (*20*). These mutants have RR spectra similar to that of WT-HPAO with C5═O stretching vibrations at 1681 and 1674 cm^{-1}, respectively (Figure 6B,C), that shift −25 and −22 cm^{-1} in $H_2{}^{18}O$ (Table 2). The course of ^{18}O exchange in D319E was monitored for 28 h to observe the slow appearance of the C5═^{18}O peak at 1656 cm^{-1} (Figure 7), yielding a $t_{1/2}$ of 3.3 h (Table 2). A somewhat faster, but still slow, rate of C5═O exchange was observed for the D319N mutant, yielding a $t_{1/2}$ of 1.6 h (Table 2). Thus, both of these mutants demonstrate a decrease of at least 40-fold in the rate of ^{18}O exchange relative to that of WT-HPAO. The markedly slower rate of C5═O exchange in the D319 mutants compared to that in WT-HPAO may be ascribed to the lower solvent accessibility of the C5═O.

Incubation of the D319E mutant in D_2O results in the appearance of a new peak at 1298 cm^{-1} (Figure 8B), indicative of a C3−D vibrational mode similar to the one observed at 1280 cm^{-1} in ECAO and at 1344 cm^{-1} in the $tBQO^-$ model. However, in the case of D319E, there is no corresponding decrease in Raman intensity at higher energy, implying that the C3−H vibration is not resonance-enhanced. Typically, C−H motions in aromatic systems gain resonance enhancement through coupling to ring vibrations that involve substantial electron delocalization in the electronic excited state. In the case of the D319E mutant, the change in frequency associated with D substitution apparently gives better energy overlap with a TPQ ring mode, thereby allowing the vibration to be observed. The D319N mutant exhibits the same behavior in D_2O with a new peak appearing at 1298 cm^{-1}, but no corresponding drop in intensity at higher energy. In both cases, exchange was complete within 60 min, the minimum time for sample preparation by ultrafiltration. The lower stability of the mutant proteins made it impossible to concentrate them to the levels required for RR detection by the dilution method. Thus, earlier reaction times could not be studied. The fact that exchange was complete at the

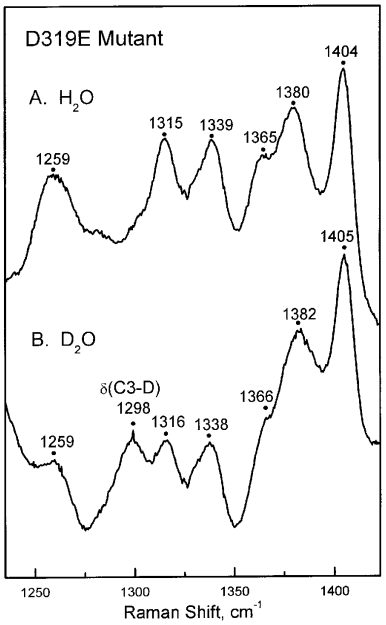

FIGURE 8: Effect of D_2O on the Raman spectrum of the D319E mutant of HPAO. (A) D319E in H_2O. (B) D319E after incubation for 86 min in 90% D_2O. Samples were 0.4 mM in TPQ, and spectra are for 15 min accumulations.

earliest 60 min time point allows us to assign a $t_{1/2}$ of <30 min for the D319 mutants (Table 2).

The pattern of slow exchange for the C5═O and fast exchange for the C3−H in both D319E and D319N suggests that the TPQ cofactor is in the flipped orientation. This interpretation is supported by an enzyme kinetics analysis of the D319E mutant in which an 80-fold reduction in the k_{cat}/K_m for methylamine was observed (*20*). Since this kinetic parameter was not affected by either substrate or solvent isotopes or viscosity, the rate limitation was best explained as being due to the need for cofactor reorientation. The flipped orientation could be stabilized by hydrogen bonding of the C2═O to E319 or N319 in the catalytic base site. However, facile C3−H exchange in the D319N mutant, which lacks a catalytic base, shows that proximity to residue 319 is not required for rapid D exchange, but rather indicates that accessibility to solvent controls the rate.

Isotope Exchange in Flanking Residue Mutants. Mutations of the residues whose side chains flank the TPQ cofactor in HPAO reveal some interesting differences in ^{18}O and D exchange rates. The E406Q mutant behaves much like WT-HPAO. The $\nu(C5{=}^{16}O)$ mode is measured at 1679 cm^{-1} (Figure 6D) and downshifts 28 cm^{-1} upon ^{18}O substitution (Table 2). The C5 carbonyl oxygen exchange was complete within 1 h, the first time point collected after reconcentration. Also, no observable C3 hydrogen exchange was detected, even after incubation for 24 h in D_2O (Table 2). Therefore, we conclude that the cofactor in the E406Q mutant is in the productive orientation, similar to that of WT-HPAO. This conclusion is in agreement with the similar rates of benzylamine oxidation in E406Q and WT-HPAO (*21*).

In the N404A mutant, the $\nu(C5{=}^{16}O)$ peak is measured at 1681 cm^{-1} (Figure 6E) and downshifts 22 cm^{-1} upon ^{18}O substitution (Table 2). The N404A mutant demonstrates a fast ^{18}O exchange, which is complete within 1 h ($t_{1/2}$ < 30 min). But, unlike the E406Q mutant, N404A also displays a fast C3 hydrogen exchange, which is complete within 1 h ($t_{1/2}$ < 30 min) as judged by the appearance of the δ(C3−D) peak at 1298 cm^{-1} upon dilution in D_2O (Table 2). These results suggest a mobile orientation of the TPQ ring in the N404A mutant, similar to that observed in ECAO. The crystal structure of WT-HPAO shows that one face of the TPQ ring lies against the amide group of Asn 404 (*8*). With Ala in place of Asn, this interaction would be lost, thus lowering the kinetic energy barrier for ring flipping and opening the active site pocket to allow for greater TPQ flexibility. Increased mobility of the TPQ ring could explain the 10^3-fold lower k_{cat}/K_m for substrate in the N404A mutant than in WT-HPAO (*17*). Furthermore, the inactivation of the N404A mutant by methylamine substrate was found to be due to the formation of a deprotonated product Schiff base whose stability was attributed to its being in a flipped orientation (*17*).

Table 3: Rates of Solvent Isotope Exchange as Indicators of Cofactor Orientation

	exchange rate[a]		TPQ orientation[b]	
enzyme	C5═O[c]	C3−H[d]	X-ray[e]	RR
HPAO	fast	no[f]	productive	productive
E406Q (HPAO)	fast	no[f]		productive
AGAO	fast	slow	ordered	productive
PSAO (pH 7.1)	fast	no[f]		productive
PSAO (pH 4.6)	slow	no[f]	flipped	flipped
D319E (HPAO)	slow	fast		flipped
D319N (HPAO)	slow	fast		flipped
ECAO	fast	fast	disordered	mobile
N404A (HPAO)	fast	fast		mobile
$tBQO^-$ model	fast	fast		mobile

[a] Fast exchange indicates a half-time of reaction of <2 min for WT enzymes and <30 min for HPAO mutants. Slow exchange indicates a half-time of reaction of 1−6 h. [b] Productive has the C5═O directed toward the catalytic base. Flipped has the C5═O directed toward Cu. Mobile can adopt either conformation. [c] C5═O exchange in $H_2{}^{18}O$ was assessed from the appearance of a new RR peak near 1650 cm^{-1}. [d] C3−H exchange in D_2O was assessed by the appearance of a new RR peak at 1290−1300 cm^{-1}. [e] From crystal structures of HPAO (*8*), ECAO (*9*), AGAO (*11*), and PSAO (*10*). [f] Not observed.

DISCUSSION

Prediction of TPQ Orientation from Exchange Rates. We have examined the C5═O and C3−H exchange rates of the TPQ cofactor for various wild-type copper-containing amine oxidases and mutant forms of HPAO. Examination of the $tBQO^-$ model compound indicates that both the C5 carbonyl oxygen and the C3 hydrogen are capable of exchanging rapidly with solvent. However, a number of these enzymes exhibit abnormally slow exchange rates ($t_{1/2}$ = 1−6 h) for either the C5═O or C3−H (Table 3). Furthermore, slow exchange on one side of the TPQ ring is generally accompanied by fast exchange ($t_{1/2} \leq$ 0.03−0.5 h) on the other side of the ring. These results can be explained by differences in solvent accessibility and suggest that the side of the TPQ ring oriented toward the substrate-binding pocket is more accessible by bulk solvent than the side oriented toward the copper center. Support for this hypothesis comes from the strong correlation between the pattern of C5═O/C3−H exchange and the TPQ cofactor orientation observed in the X-ray crystal structure. Thus, in the amine oxidases that were examined, the exchange rates determined by RR spectroscopy serve to differentiate between productive, flipped, and mobile orientations of the TPQ cofactor.

The *productive* orientation of TPQ, with its C5 carbonyl oxygen near the substrate-binding site and its C3 hydrogen near the bound Cu, has been observed in the crystal structure of WT-HPAO (*8*). The resting enzyme exhibits rapid C5═O exchange, as expected, with the C3−H exchange being either exceedingly slow or not observable due to a lack of resonance enhancement (Table 3). The same pattern of fast C5═O exchange and a nonobservable C3−H exchange are seen for PSAO at pH 7.1 and for the E406Q mutant of HPAO. Although no crystal structures are available for these proteins, our prediction of a productive orientation is supported by their high enzymatic activities. Finally, AGAO shows the definitive pattern of a productive orientation with fast C5═O exchange and slow C3−H exchange (Table 3). Although the orientation of the TPQ ring in AGAO has not been verified by X-ray crystallography because of the difficulty of locating the carbonyl oxygens (*11*), the ring itself has well-defined electron density suggestive of an ordered rather than a mobile cofactor.

The *flipped* orientation of TPQ, with its C5 carbonyl oxygen directed toward the Cu-binding site and its C3 hydrogen facing the substrate-binding pocket, has been observed in the crystal structure of PSAO at pH 4.8 (*10*). As expected for a flipped orientation, the rate of C5═O exchange in PSAO at pH 4.6 is 135-fold slower than at pH 7.1 (Table 2) and is also much slower than that of the $tBQO^-$ model at pH 4. These results are consistent with a buried environment for the C5═O and flipped designation for TPQ in low-pH PSAO (Table 3). The lack of a RR vibrational mode for the C3 hydrogen or C3 deuterium makes it impossible to determine whether the C3 hydrogen has the expected fast rate of exchange in low-pH PSAO. However, the D319E and D319N mutants of HPAO do exhibit both of the predicted characteristics of a flipped cofactor orientation: slow C5═O exchange and fast C3−H exchange (Table 3). The low-pH form of PSAO and the D319E mutant of HPAO also exhibit reduced enzymatic reaction rates, consistent with the need for cofactor reorientation.

The D319E mutant of HPAO turns over methylamine and phenethylamine substrates 80- and 15-fold more slowly, respectively, than WT-HPAO, whereas the D319N mutant of HPAO has no catalytic activity (*20*). The fact that D319E is still active toward substrates and that the reaction is faster than the rate of C5═O exchange with solvent implies that the TPQ cofactor flips back to a productive conformation in the presence of substrate to initiate substrate turnover (*20*). Furthermore, an extensive kinetic analysis of D319E revealed that the decreased rate of reaction with substrate is due to a rate-limiting conformational change (*20*). Additionally, D319N was shown to form a covalent adduct with ammonium chloride similar to the adduct formed with D319E reacted with methylamine. Both of these adducts were identified as deprotonated iminoquinones by RR spectroscopy (*20*) and ascribed to a deprotonation process that accompanies the flipping of the TPQ ring. A flipped iminoquinone complex would be expected to hydrolyze slowly due to a lack of solvent accessibility to the backside of the TPQ ring. A large solvent isotope effect was, in fact, observed for k_{cat} for the oxidation of methylamine by D319E and attributed to a rate-limiting hydrolytic step (*20*). These kinetic results support our conclusion that the TPQ cofactor in the D319E and D319N mutants of HPAO has enhanced stability in the flipped orientation. Unexpectedly, the similarity of solvent exchange rates for D319E and D319N rules out the possibility that the catalytic base is essential for either C3−H or C5═O exchange, consistent with the fast rates observed for uncatalyzed exchange in the $tBQO^-$ model compound (*18*).

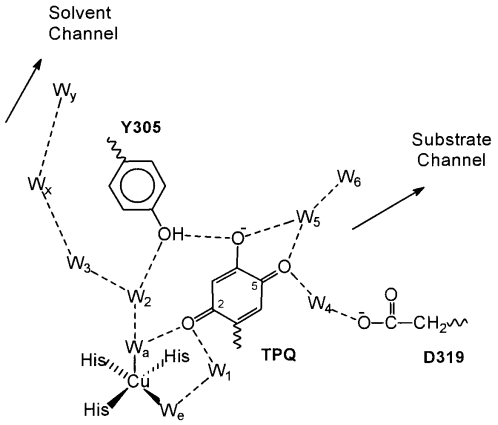

FIGURE 9: Immobilized water molecules in the active site of HPAO as detected in the crystal structure at 2.4 Å resolution (adapted from ref *8*). Dashed lines represent hydrogen bonds 2.4−3.0 Å in length, except for W_x and W_y at 4.2−4.9 Å.

A *mobile* cofactor with the TPQ ring adopting a multitude of conformations is suggested by the crystal structure of ECAO with its weak electron density for the TPQ ring (*9*). The C5═O and C3−H fast exchange rates in ECAO support this conclusion (Table 3). The N404A mutant of HPAO shows a similar pattern of rapid C5═O and C3−H exchange indicating that it, too, has a mobile cofactor. It has been previously proposed that the Asn 404 side chain lies against one face of the TPQ ring in WT-HPAO, providing conformational constraints during catalytic turnover (*17*). Thus, it is understandable why conversion of this Asn to Ala would increase cofactor mobility.

There are limitations to X-ray crystallography, which include the difficulty in observing accurate electron densities in large molecule structures and the potential difference between enzyme conformational states in the crystal versus the enzyme in solution. Although the high-resolution (2.0 Å) structure for ECAO showed well-defined electron densities for other aromatic rings and amino acid residues, the TPQ cofactor ring was disordered (*9*). This indicates that the resolution was sufficient to distinguish the full electron density for the TPQ ring and, thus, implicates cofactor mobility as the source of poor electron density for TPQ. Furthermore, these crystals were shown to be catalytically competent (*25*), consistent with a similar behavior for TPQ in the crystalline and solution states.

Structural Basis for Differences in Exchange Rates. The crystal structure of HPAO identifies a large substrate channel leading from the solvent-accessible surface to the active site base (Figure 9; *8*). A bridging water molecule, W_4, between the C5 carbonyl oxygen and the aspartate base is very near the edge of the substrate channel, immobilized water molecules W_5 and W_6 are contained within the identified substrate channel, and all are expected to be able to be displaced by substrate binding. The fact that these water molecules have defined and identical locations in the six independent subunits that comprise the asymmetric unit (*8*) suggests that they

constitute a part of the protein structure in the resting enzyme. Additionally, however, there is disordered solvent that is expected to comprise the bulk of the substrate channel and to be within close proximity of the C5═O. The side of the TPQ ring oriented toward the substrate-binding site would, thus, be positioned for rapid exchange.

On the Cu side of the active site in HPAO, the crystal structure identified a chain of five immobilized water molecules (Figure 9). This chain begins with the axial copper ligand W_a and continues through W_2, W_3, and W_x. The fifth water (W_y) is hydrogen bonded to a cluster of solvent molecules in another solvent-accessible cavity (*8*). This chain of water molecules is conserved for subunit B of the 2-hydrazinopyridine complex of ECAO (*13*) and is conserved from the W_2 position on for the zinc-substituted HPAO (*26*). Although the immobilized waters are potentially solvent exchangeable, the distance to this other solvent-accessible channel in HPAO is quite large, on the order of 15 Å (from the TPQ ring). The extensive and conserved nature of the H-bonding chain suggests that it is stabilized by the protein environment and is essentially part of the protein structure. Such environmental effects have been well-documented for the bovine pancreatic trypsin inhibitor where the rate of amine NH exchange with solvent was found to decrease as much as 10^5-fold for buried amides due to hydrogen bonding and/or a lack of solvent accessibility (*27*). Thus, it is possible that the slow C3−H or C5═O exchange rates when they are located on the Cu side of the active site (Figure 9) are due to this site having reduced accessibility to bulk solvent.

Functional Significance of Cofactor Mobility. The ability of the TPQ cofactor to access catalytically nonproductive orientations would appear to be counterproductive for normal enzyme activity. However, copper amine oxidases are unique enzymes in that they self-catalyze the biogenesis of their own organic cofactor, as well as providing catalytic activity for the oxidative deamination of primary amine substrates. Cofactor biogenesis has been proposed to begin with a copper-facilitated oxygenation at the C5 position, followed by ring flipping and a copper-facilitated hydroxylation at the C2 position (*7*, *21*). Thus, the TPQ precursor ring must be able to rotate through 180° to allow access of both sides of the ring to the Cu site. The ability to incorporate ^{18}O at the C2 position (ref *25* and this work) shows that the Cu-binding site is fully accessible to solvent in the apoenzyme. Since only the productive TPQ orientation is expected to promote catalysis, stabilization of this orientation presumably accompanies TPQ formation or substrate binding in the WT enzyme. As described elsewhere (*16*, *17*, *20*) and herein, selected active site mutants of HPAO have increased cofactor mobility with a corresponding decrease in catalytic activity.

ACKNOWLEDGMENT

We are grateful to Drs. Hans Duine and Vincent Steinebach for providing samples of ECAO, Dr. Katsuyuki Tanizawa for providing samples of AGAO, Dr. Doreen Brown for providing samples of PSAO, Drs. Julie Plastino, Benjamin Schwartz, and Joanne Dove for providing the HPAO mutants, and Dr. Minae Mure for providing the $tBQO^-$ model compound.

REFERENCES

1. McIntire, W. S., and Hartman, C. (1993) in *Principles and Applications of Quinoproteins* (Davidson, V. L., Ed.) pp 97−171, Marcel Dekker, New York.
2. Salmi, M., Yegutkin, G. G., Lehvonen, R., Koskinen, K., Salminen, T., and Jalkanen, S. (2001) *Immunity 14*, 265−276.
3. Janes, S. M., Mu, D., Wemmer, D., Smith, A. J., Kaur, S., Maltby, D., Burlingame, A. L., and Klinman, J. P. (1990) *Science 248*, 981−987.
4. Choi, Y. H., Matsuzaki, R., Fukui, T., Shimizu, E., Yorifuji, T., Sato, H., Ozaki, Y., and Tanizawa, K. (1995) *J. Biol. Chem. 270*, 4712−4720.
5. Dove, J. E., Schwartz, B., Williams, N. K., and Klinman, J. P. (2000) *Biochemistry 39*, 3690−3698.
6. Ruggiero, C. E., Smith, J. A., Tanizawa, K., and Dooley, D. M. (1997) *Biochemistry 36*, 1953−1959.
7. Ruggiero, C. E., and Dooley, D. M. (1999) *Biochemistry 38*, 2892−2898.
8. Li, R., Klinman, J. P., and Matthews, F. S. (1998) *Structure 6*, 293−307.
9. Murray, J. M., Saysell, C. G., Wilmot, C. M., Tambyrajah, W. S., Jaeger, J., Knowles, P. F., Phillips, S. E. V., and McPherson, M. J. (1999) *Biochemistry 38*, 8217−8227.
10. Kumar, V., Dooley, D. M., Freeman, H. C., Guss, J. M., Harvey, I., McGuirl, M. A., Wilce, M. C., and Zubak, V. M. (1996) *Structure 4*, 943−955.
11. Wilce, M. C., Dooley, D. M., Freeman, H. C., Guss, J. M., Matsunami, H., McIntire, W. S., Ruggiero, C. E., Tanizawa, K., and Yamaguchi, H. (1997) *Biochemistry 36*, 16116−16133.
12. Wilmot, C. M., Hajdu, J., McPherson, M. J., Knowles, P. F., and Phillips, S. E. V. (1999) *Science 286*, 1724−1728.
13. Wilmot, C. M., Murray, J. M., Alton, G., Parsons, M. R., Convery, M. A., Blakeley, V., Corner, A. S., Palcic, M. M., Knowles, P. F., McPherson, M. J., and Phillips, S. E. V. (1997) *Biochemistry 36*, 1608−1620.
14. Mure, M., and Klinman, J. P. (1995) *J. Am. Chem. Soc. 117*, 8698−8706.
15. Mure, M., and Klinman, J. P. (1995) *J. Am. Chem. Soc. 117*, 8707−8718.
16. Cai, D., Dove, J., Nakamura, N., Sanders-Loehr, J., and Klinman, J. P. (1997) *Biochemistry 36*, 11472−11478.
17. Schwartz, B., Green, E. L., Sanders-Loehr, J., and Klinman, J. P. (1998) *Biochemistry 37*, 16591−16600.
18. Moënne-Loccoz, P., Nakamura, N., Steinebach, V., Duine, J. A., Mure, M., Klinman, J. P., and Sanders-Loehr, J. (1995) *Biochemistry 34*, 7020−7026.
19. Nakamura, N., Matsuzaki, R., Choi, Y., Tanizawa, K., and Sanders-Loehr, J. (1996) *J. Biol. Chem. 271*, 4718−4724.
20. Plastino, J., Green, E. L., Sanders-Loehr, J., and Klinman, J. P. (1999) *Biochemistry 38*, 8204−8216.
21. Schwartz, B., Dove, J. E., and Klinman, J. P. (2000) *Biochemistry 39*, 3699−3707.
22. McGuirl, M. A., McCahon, C. D., McKeowan, K. A., and Dooley, D. M. (1994) *Plant Physiol. 106*, 1205−1211.
23. Loehr, T. M., and Sanders-Loehr, J. (1993) *Methods Enzymol. 226*, 431−470.
24. Wang, S. X., Nakamura, N., Mure, M., Klinman, J. P., and Sanders-Loehr, J. (1997) *J. Biol. Chem. 272*, 28841−28844.
25. Nakamura, N., Moënne-Loccoz, P., Tanizawa, K., Mure, M., Suzuki, S., Klinman, J. P., and Sanders-Loehr, J. (1997) *Biochemistry 36*, 11479−11486.
26. Chen, Z., Schwartz, B., Williams, N. K., Li, R., Klinman, J. P., and Mathews, F. S. (2000) *Biochemistry 39*, 9709−9717.
27. Wagner, G., and Wüthrich, K. (1982) *J. Mol. Biol. 160*, 343−361.

BI011685Y